ELSEVIER

Contents lists available at ScienceDirect

# Microchemical Journal

journal homepage: www.elsevier.com/locate/microc





# Advanced characterization in molecularly imprinted Polypyrrole for potentiometric lactose sensing

C. Perez-Gonzalez <sup>a,b</sup>, C. Garcia-Hernandez <sup>a,b,\*,1</sup>, C. Garcia-Cabezon <sup>a,b,\*,2</sup>, M.L. Rodriguez-Mendez <sup>b,c</sup>, F. Martin-Pedrosa <sup>a,b</sup>

- <sup>a</sup> Dpt. of Materials Science, Universidad de Valladolid, Paseo del Cauce, 59, 47011 Valladolid, Spain
- <sup>b</sup> BioecoUVA Research Institute, Universidad de Valladolid, 47011 Valladolid, Spain
- <sup>c</sup> Dpt. of Inorganic Chemistry, Universidad de Valladolid, Prado de la Magdalena, s/n, 47011 Valladolid, Spain

# ARTICLE INFO

# Keywords: Molecularly imprinted polymers (MIPs) Polypyrrole (PPy) Potenciometric sensor Electrochemical characterization Surface characterization Lactose

#### ABSTRACT

The motivation behind this study comes from the necessity to monitor lactose levels in milk for quality control and public health, as existing methods are often complex, time-consuming, and expensive. This research aims to develop a specific and sensitive potentiometric sensor for lactose detection using electropolymerised polypyrrolebased molecularly imprinted polymers (MIPs). MIP sensors were developed through chronoamperometric electropolymerisation of pyrrole in the presence of lactose, creating specific binding sites. Raman spectroscopy, Scanning Electron Microscopy (SEM), and Atomic Force Microscopy (AFM) were used to assess surface morphology confirming the presence of imprinted cavities and surface changes after lactose removal. The electrochemical performance of the sensors was evaluated by EIS spectroscopy demonstrating the influence of MIP cavities on the electron transfer of the sensor compared to non-imprinted polymer (NIP). Finally, open circuit potentials (OCP) in various lactose concentrations and real milk samples confirmed the high sensitivity and selectivity of the MIP sensors. Moreover, Principal Component Analysis (PCA), Partial Least Square Regression (PLS), and Support Vector Machine (SVM) models were satisfactorily employed to establish correlations between OCP measurements and lactose content, allowing its prediction in milk samples with an average error of 6 %. The results demonstrated that the MIP sensors exhibited high selectivity and sensitivity towards lactose, with improved responses compared to NIP sensors. The study concludes that polypyrrole-based MIPs provide a robust and effective approach for lactose detection and prediction in dairy products, offering a promising tool for quality control and ensuring consumer safety.

# 1. Introduction

Lactose, the main disaccharide sugar found in milk, plays a crucial role in the dairy industry. Lactose content significantly affects the taste, texture, and fermentation process of dairy products, influencing overall quality and consumer acceptance [1]. Accurate lactose quantification is also required to produce lactose-free and low-lactose products, which are in high demand due to a recent rise in lactose intolerance cases worldwide [2,3]. Additionally, precise lactose quantification is required to comply with food labelling regulations and standards, ensuring product safety and health compliance. In the industry, efficient lactose monitoring also contributes to waste reduction, process optimization,

and increased economic efficiency [4]. Therefore, it is essential to use sophisticated analytical methods for lactose measurements.

Electrochemical techniques present an attractive alternative to traditional techniques [5–7] due to their rapid and sensitive detection capabilities using relatively simple and low-cost instrumentation [8,9]. Within the realm of electrochemical sensors, potentiometric sensors offer distinct advantages. They are particularly noted for their simplicity, low power requirements, and the ability to provide real-time measurements. Potentiometric sensors measure the potential difference between a working electrode and a reference electrode, which is related to the concentration of the analyte by the Nernst equation. This method allows for quick and precise detection without the need of extensive

https://doi.org/10.1016/j.microc.2025.114709

<sup>\*</sup> Corresponding authors at: Dpt. of Materials Science, Universidad de Valladolid, Paseo del Cauce, 59, 47011 Valladolid, Spain. E-mail addresses: celia.garcia.hernandez@uva.es (C. Garcia-Hernandez), crigar@eii.uva.es (C. Garcia-Cabezon).

<sup>&</sup>lt;sup>1</sup> Orcid: 0000–0002–2444-2204.

<sup>&</sup>lt;sup>2</sup> Orcid: 0000-0003-0524-5931.

sample preparation [10-13].

Biosensors, which utilize biological recognition elements like enzymes or antibodies, provide a viable option for lactose detection due to their high sensitivity, selectivity, potential for miniaturization, and ability for real-time, label-free detection in food processing environments [14–17]. However, biosensors that rely on enzyme, aptamer or antibody-based receptors face significant challenges, such as limited shelf-life and instability under testing conditions, which can hinder their widespread adoption [18].

Molecular imprinted polymers (MIPs) are polymeric materials designed and produced with built-in molecular recognition sites. This essential characteristic has led to an increasing interest in their development as strong, low-cost materials with sensitive and specific chemical recognition capability. As an alternative sensing material for biosensors, MIPs have proven to have several significant benefits, such as being simple to prepare, stable in storage, inexpensive, able to be used repeatedly without losing functionality, highly mechanically strong, and resistant to extreme conditions in temperature, pressure, and chemical environments [19]. Typically, the MIP method enables the polymerization of a functional monomer in the presence of target molecules (referred to as templates) to create particular molecular recognition sites. After removing the template, the particular recognition cavities are revelled [20]. Conversely, the MIPs selectivity is confirmed by the nonimprinted polymers (NIPs), which were made using the same procedures but without a template and lack any particular recognition abilities [21].

Molecularly imprinted polymers (MIPs) are commonly synthesized using two main methods: covalent and non-covalent imprinting. The covalent approach forms strong, specific bonds between the monomer and the template, resulting in highly selective binding sites. However, this method can be limited by the slow binding and release of the target molecule due to the need to form and break covalent bonds. In contrast, the non-covalent method relies on weaker interactions, such as hydrogen bonds and van der Waals forces, making the synthesis process simpler and allowing for faster binding and release of the target molecule. Despite the potential for less stable and non-stoichiometric monomer-template complexes, the non-covalent approach remains the most widely used due to its operational simplicity [22].

Futhermore, while MIPs offer high selectivity and robustness, their application in complex food matrices such as milk, wine, and fruit juices remains challenging due to issues such as matrix effects, nonspecific binding, and fouling of the sensor surface [23]. These challenges can interfere with the recognition performance of the MIP, reduce signal reliability, and complicate calibration procedures [24]. For example, milk contains a wide range of interfering components—such as proteins, fats, and salts—that can non-specifically adsorb onto the polymeric surface or hinder the diffusion of the target analyte into the imprinted cavities [24–26]. Additionally, the high viscosity and complex composition of such matrices can lead to sensor fouling and decreased sensitivity [27].

Some studies have reported successful integration of MIPs into potentiometric platforms for analyte detection in real food samples, including histamine in wine [28], urea in milk [29], and flavonoids in juices [30,31], highlighting both the potential and current limitations of these systems in real-world applications [32].

The fabrication of these sensors typically involves incorporating the MIP receptor into a polymeric sensing membrane, dispersing MIP particles in a plasticizer, and embedding the mixture in a polyvinyl chloride (PVC) film [22,33,34]. Other methodologies include, embedding MIPs particles in pastes or inks [35] creating template-compatible sites on indium tin oxide (ITO) glass plates [36], embedding MIPs particles in carbon paste electrodes [37] or developing glassy membranes as transistors [38].

Electropolymerisation is a widely used method for preparing MIP-based electrochemical sensors due to its simplicity, cost-effectiveness, and ability to create polymeric layers with controlled thickness, high sensitivity and rapid response. There are two ways to carry out the

electropolymerisation process: reduction or oxidation. The most widely utilized technique for generating conductive polymer is oxidation [39,40]. Among many conducting polymers used in electropolymerisation, polypyrrole stands out due to its high electrical conductivity, suitable redox properties, good biocompatibility, and ease of polymerization compared to other conducting polymers such as polyaniline [41], polythiophene [42] poly(o-phenylenediamine) [43,44], poly(o-aminophenol) [45] or poly-nicotinamide [46]. These properties make polypyrrole an excellent candidate for developing sensitive and selective electrochemical sensors [47–49].

Several studies have demonstrated the successful application of polypyrrole in potentiometric sensors. For example, potentiometric sensors based on polypyrrole have been developed for the detection of various ions, such as nitrate [50], phosphate [51], chloride and ammonium [40] showcasing their versatility and efficiency. However, there are very few examples of potentiometric sensors based on polipyrrole and MIPs applied in the dairy industry compared with voltammetric techniques where polypyrrole-based MIPs have been employed in the detection of mastitis markers [52,53] antibiotics [54,55], allergens [56] and toxins [57].

This study aims to develop a specific and sensitive detection system for lactose using electropolymerised polypyrrole-based MIP potentiometric sensors. Moreover, RAMAN spectroscopy, Scanning Electron Microscopy (SEM) and Atomic Force Microscopy (AFM) were used to characterize the sensors surface changes between MIPs and NIPs. The molecular imprinted polymer was characterized by EIS and potentiometric electrochemistry to ensure its selectivity and sensitivity towards lactose content in real milk samples. By leveraging the unique properties of MIPs and the advantages of polypyrrole as the sensor matrix, this research seeks to advance the field of electrochemical sensing in dairy product analysis and quality control, providing a robust tool for ensuring product safety.

#### 2. Materials and methods

# 2.1. Reagents and solutions

All chemicals and solvents were of reagent grade and used without further purification. The solutions were obtained by solving substances in deionized water (resistivity of  $18.2\,\mathrm{M}\Omega\cdot\mathrm{cm}^{-1}$ ) obtained from a Milli-Q system (Millipore). Pyrrole, 1-decanesulfonate (DSA), potassium chloride, sodium hydroxide and lactose were purchased from Sigma-Aldrich.

# 2.2. Milk samples

The samples analysed in this work were 14 local cow milk samples from the region of Castilla y León (Spain). The set of samples was sorted by their lactose content (high —H—, medium -M- and low -L- content) that was analysed using the standard HPLC chemical method according with the international standardised methods. Table 1 collects the lactose content of the milk samples under study.

# 2.3. Sensors fabrication

The fabrication of the sensors was carried out using an electropolymerisation method, specifically chronoamperometry, at room temperature using Solartron 1285 A potentiostat/galvanostat (Oak Ridge, TN, U.S.A.) applying 1.2 V during 300 s. A three-electrode configuration cell was used with a counter electrode of graphite, the reference electrode of Ag|AgCl in a 3 mol·L $^{-1}$  KCl solution and a working electrode of gold (Au) (3.0 mm diameter, 99.95 % purity) from BASI (West Lafayette, IN, USA).

# 2.3.1. Molecularly imprinted polypyrrole film electrode (MIP electrodes)

To modify the Au working electrode with a molecularly imprinted polypyrrole PPy/DSA film, the BASI electrode was placed in an aqueous  $\,$ 

**Table 1**Milk samples analysed with their lactose content.

	Nomenclature	Lactose content (% w/w)
High content	1H	5.48
	2H	5.40
	3H	5.29
	4H	5.21
Medium content	1 M	5.11
	2 M	4.89
	3 M	4.78
	4 M	4.76
	5 M	4.66
	6 M	4.44
Town content	1.7	4.00
Low content	1 L	4.03
	2 L	4.21
	3 L	3.80
	4 L	3.37

solution of 0.1 mol·L $^{-1}$  Py as monomer and 0.05 and mol·L $^{-1}$  DSA as dopant containing 5·10 $^{-3}$  mol·L $^{-1}$  of lactose as template molecule. Electropolymerizations were carried out using a Parstat 2273 potentiostat/galvanostat (EG&G, Oak Ridge, TN, USA). The disks were polished with 120 grit paper and rinsed with deionized water in an ultrasonic bath. The auxiliary electrode was a conventional Pt electrode. The reference electrode was an Ag/AgCl electrode in a 3 mol/L KCl solution. The electropolymerisation process was performed by chronoamperometry using 1.2 V during 300 s, potential and time conditions were selected on the basis of previous work by the authors [58,59]. Next, the electrodes were immersed in a solution of 0.1 mol·L $^{-1}$  NaOH for 30 min under stirring conditions to reveal the imprinted cavities by removing the lactose template molecule from the polymeric structure. Thereafter, the lactose MIP electrode based on PPy/DSA is completed.

During the electropolymerization of polypyrrole in the presence of lactose, molecular interactions occur between the pyrrole monomers and the lactose molecules. These interactions are predominantly noncovalent, involving hydrogen bonding between the hydroxyl groups of lactose and the nitrogen atoms in the pyrrole rings. As the polymerization progresses, the growing polypyrrole matrix entraps the lactose molecules, effectively embedding them as templates. Subsequently, the electrodes are treated with a NaOH solution, which disrupts these interactions and removes the lactose, leaving behind imprinted cavities that are spatially and chemically complementary to the lactose molecule. These recognition sites can selectively rebind lactose during sensing, altering the interfacial charge distribution and, consequently, the open circuit potential (OCP) measured by the sensor. This noncovalent imprinting approach has been previously reported in the literature for the preparation of MIPs in potentiometric sensors [22] [34] [60] [61].

# 2.3.2. Non-molecularly imprinted polypyrrole film electrode (NIP electrodes)

The Au BASI electrodes were modified with PPy/DSA film using the same experimental procedure above described in the absence of lactose to create non-molecularly imprinted polymer electrodes for comparison purposes.

# 2.4. Sensors characterization

The electrochemical characterization of the sensors was carried out using a Solartron 1285 A potentiostat/galvanostat (Oak Ridge, TN, U.S. A.) to record the open circuit potentials (OCP). For each measurement, the electrodes were first immersed for 1800 s under stirring conditions in aqueous solutions containing the target analyte (lactose, glucose and galactose) at the desired concentrations. After this pre-incubation step,

the electrodes were rinsed with deionized water and transferred to a 0.1  $\rm mol \cdot L^{-1}$  KCl solution, where the OCP was recorded for 1800 s at room temperature. The electrochemical impedance spectroscopy (EIS) was conducted with a Solartron 1260 A impedance gain-phase analyser (West Sussex, UK) to obtain Bode plots in 0.1  $\rm mol \cdot L^{-1}$  KCl by applying 10 mV signal amplitude on frequencies ranging from 0.1 to  $10^5$  Hz. All experiments were carried out in five replicates.

The Raman spectra were measured with a portable Raman BWTEK modular spectrometer coupled to a microscope (Plainsboro, NJ, USA). The spectrometer is equipped with a detector BWTEK Exemplar-Pro (resolution of 4 cm<sup>-1</sup>) and a laser excitation source BWTEK CleanLaze (Power Output 10-940 mW and 785 nm laser excitation wavelength). The equipment was calibrated with the  $\nu(\text{Si} - \text{Si})$  vibration mode, located at 520.7 cm<sup>-1</sup>, of a Si standard. The acquisition times were 80-60 s, and the laser power was adjusted to 500 mW, as higher values shall burn the samples. The magnification employed with the microscope was ×20. A SEM-FEI (QUANTA 200F) was used to observe the microscopic structure of the working electrode surfaces and confirm the creation of the imprinted cavities. In addition, the sensors topography was analysed using Atomic force microscopy (AFM) using a Cypher ES Environmental AFM device operating in tapping mode with blue drive photothermal and an AC160TSA-R3 tip (Oxford Instruments, Asylum Research, Wiesbaden, Germany).

# 2.5. Electroanalytical measurements in milk samples

The milks were analysed using the OCP responses of the MIP and NIP electrodes in 0.1  $\rm mol\cdot L^{-1}$  KCl for 1800 s at room temperature after being immersed in milk samples with different lactose content under stirring for 1800 s.

# 2.6. Statistical analysis

The statistical analysis was performed by using The Unscrambler v9.7. (Oslo, Norway) and Orange Data Mining (University of Ljubljana, Slovenia). Principal Component Analysis (PCA) was used to evaluate the discrimination capability of the MIP and NIP electrodes. Partial Least Square Regression-1 (PLS-1) was used to establish correlations between the results obtained from the electrodes in milk samples and their lactose content. Finally, Support Vector Machine (SVM) was used to predict the lactose content of milk samples using the electroanalytical OCP measurements.

# 3. Results and discussion

# 3.1. Sensors characterization

The structure and composition of MIP and NIP electrodes were investigated by Raman spectra, Fig. 1 shows the spectra of MIP before and after NaOH washing, as well as NIP. The Raman spectrum for nonimprinted PPy has seven significant bands located at 919, 979, 1046, 1320, 1401, 1485 y 1579 cm<sup>-1</sup>. The strong peak located at approximately 1579 cm<sup>-1</sup> corresponds with C—C backbone stretching. The smaller peaks at 919, 979 and 1046 cm<sup>-1</sup> are associated to C—H in plane deformation of PPy. The peak at 1320 cm<sup>-1</sup> is attributed to ring stretching, the peak at 1401 cm<sup>-1</sup> to C—C in plane deformation and the peak at 1485 cm<sup>-1</sup> to vibration ring. The peak at 934 cm<sup>-1</sup> was significantly enhanced in the spectrum of MIP and a new peak at 1082 cm<sup>-1</sup> appeared. Comparing the Raman spectra before and after washing, the first peak decreased in intensity and the last one disappeared. According to the literature [62], these peaks could be associated to an O-C-O bending and the stretching vibration of the bridge C-O-C group, respectively, of lactose. The spectrum of MIP after washing is similar to that of NIP which also proves the removal of the lactose template from PPy films. Raman analysis indicates a successful modification of PPy on the surface.

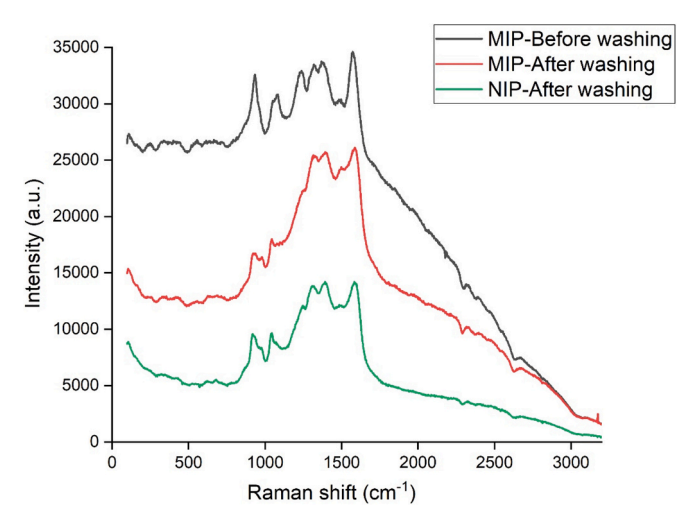


**Fig. 1.** Raman spectra of PPy for non-imprinted PPy films and imprinted PPy films before and after washing.

SEM analyses were performed to study the surface morphology of electropolymerised film on surface electrodes and the particle size of the NIP and MIP electrodes before and after the removal of lactose (Fig. 2a, b, c y d). The typical cauliflower-like structure of polypyrrole is observable in all cases. However, significant differences are observed between the two electrodes both before and after removal and oxidation treatment with NaOH. From the images, it seems that the polymer spatial distribution is homogeneous for both electrodes, but the MIP (Fig. 2a) shows a clearly smaller particle size than NIP (Fig. 2c). This suggests that lactose (some particles are still visible on the MIP surface) interferes with the electropolymerisation. Prior to the removal of lactose, the particle size was observed to be small and regular in both,

compared to after washing the imprinted polymer, when the particle size changed to thick and globular (Fig. 2.a and Fig. 2b). The granular structure of polypyrrole is preserved even after the washing and oxidative treatment. However, the MIP appeared rough and irregular with more spaces between polymer particles, and these properties may be attributed to the formation of the recognizing cavities. Similar SEM results have been reported for MIP electrodes [63], A morphological study of molecularly imprinted polymers using the scanning electron microscope [64] and reported similar SEM results for molecularly imprinted polymers [65].

The topography of the MIP electrodes before and after washing was probed using AFM (Fig. 3). In both cases, a uniform, granular structure, with different grain size is observed. The AFM-3D scans show the granular structure consistent with the cauliflower morphology observed by the SEM, greater chemical heterogeneity was observed in the MIP sample before washing, which could be related to the presence of lactose. The AFM allows for the measurements of average roughness (Ra) and root mean square (RMS), and consequently, the evaluation of the surface of each layer in the construction of the MIP sensor [66]. The Ra and RMS of MIP-Lactose (before washing) were 103.29 and 131.9 nm, showing a rough morphology related to the successful deposition of the polymeric film. The extraction of the lactose from the MIP causes a significant structural change, as revealed by the image. The topography is even rougher, while the Ra and RMS increases to 189.5 and 246.9 nm, supporting the extraction procedure. The process removes the lactose, creating imprinted cavities that leads to an increase in roughness [67]. Also, the surface height is increased after removal of lactose due to the vacant recognition sites leading to a higher surface area.

# 3.2. Electrodeposition and electrochemical characterization of sensors

Characterizing the electrochemical properties of MIP sensors from their construction to their application in detecting the target molecule is

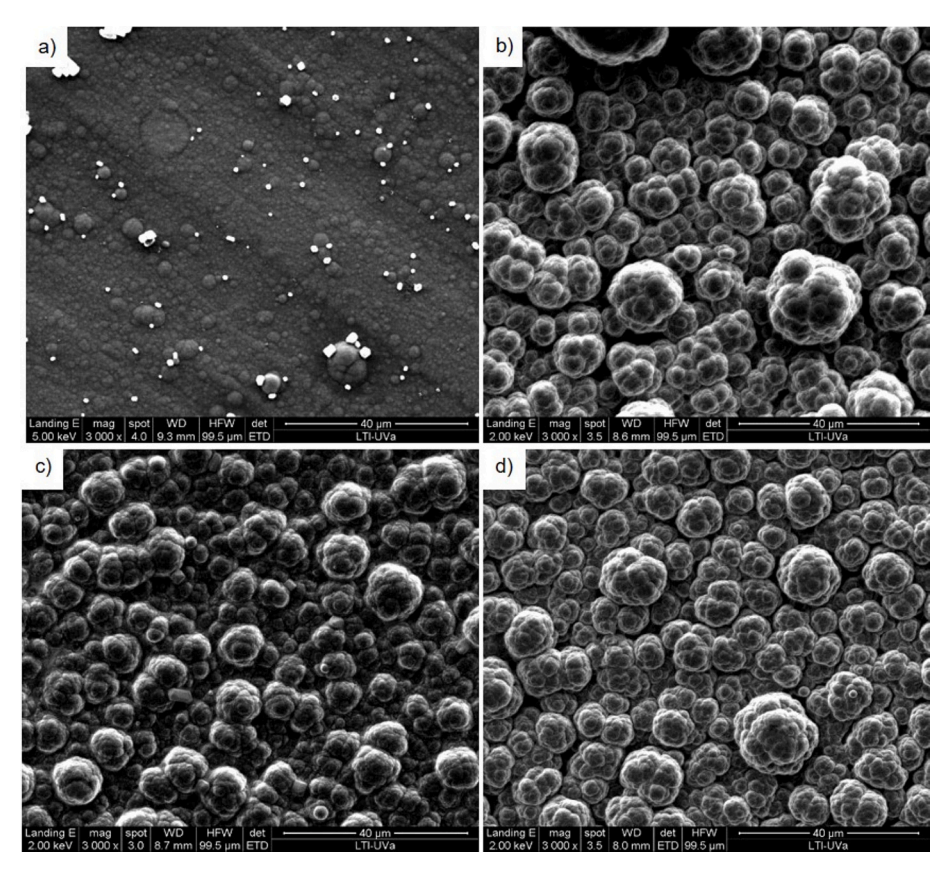


Fig. 2. SEM images of Au electrodes coated with the PPy-MIP (a) before and (b) after washing and PPy-NIP (c) before and (d) after washing fims.

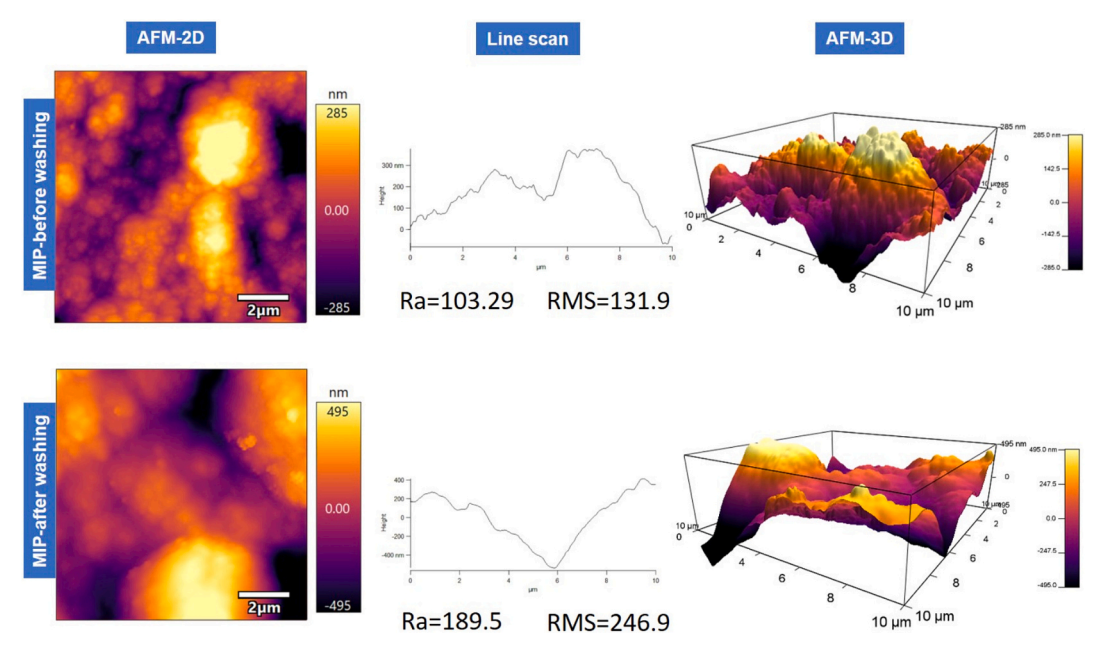


Fig. 3. AFM, 2D maps, line scans and 3D images of PPy-MIP films before and after washing.

essential for understanding their performance and specificity. This process includes examining the electrodeposition of the polymer, the response to the target molecule, and the subsequent washing steps to ensure proper functioning and selectivity of the sensor.

Fig. 4 shows the chronoamperometry electrodeposition of the polypyrrole-DSA and the OCP response in KCl  $0.1~{\rm mol \cdot L^{-1}}$  over time for both sensors (MIP and NIP). A display of the current signals during the electrodeposition is showed in Fig. 4a. After a short induction period where diffusion controls the monomer oxidation, the current increased rapidly with time, where polymer started nucleating and growing on the electrode surface. Finally, the current reached a plateau coinciding with a continuous and gradual polymer growth. The increase in the current intensity during the electrodeposition of the MIP, compared to the NIP, suggests that the presence of lactose molecules during polymerization enhances the conductivity of the polypyrrole and facilitates the formation of efficient, specific cavities, thereby creating more reactive sites for the target molecule.

On the other hand, Fig. 4b represents the MIP sensor OCP signals with the target molecule still within the polymer, and after washing the sensor with NaOH to elute the target molecule from the polymer (MIPwashed). As it can be observed, following the washing step with NaOH, the potential decreases, reflecting the elution of the target molecule.

Fig. 4c illustrates the OCP signals for the NIP sensor through similar stages: after electrodeposition without the target molecule, and after washing with NaOH. The potential is lower than the obtained with the MIP both before and after washing. The higher OCP suggests that the MIP has a more organized and higher energy surface state due to these specific cavities, which can still affect the potential even without the presence of the target molecule, lactose. This phenomenon underscores the successful creation of the molecular imprints within the polymer matrix [68].

Useful information on the modifications at the electrode/electrolyte interface was also delivered by EIS method. Fig. 5 shows the Bode diagrams obtained for bare substrate, NIP electrode and MIP electrodes before and after washing. In all cases, the modulus of impedances in the high-frequency region is related to the resistance of the electrolyte, while in the low-frequency region it correlates to the resistance to electronic transfer of electrode. After the electropolymerisation process, an increase was observed in impedance module at low frequencies for both non-imprinted (curve b) and imprinted (curve c) electrodes, compared to the bare substrate (curve a). This shows that the PPy polymeric film on the bare surface restricted the charge-transfer at the electrode-solution interface. MIP electrode (curve c) showed a higher impedance modulus than the NIP electrode (curve b), indicating that the

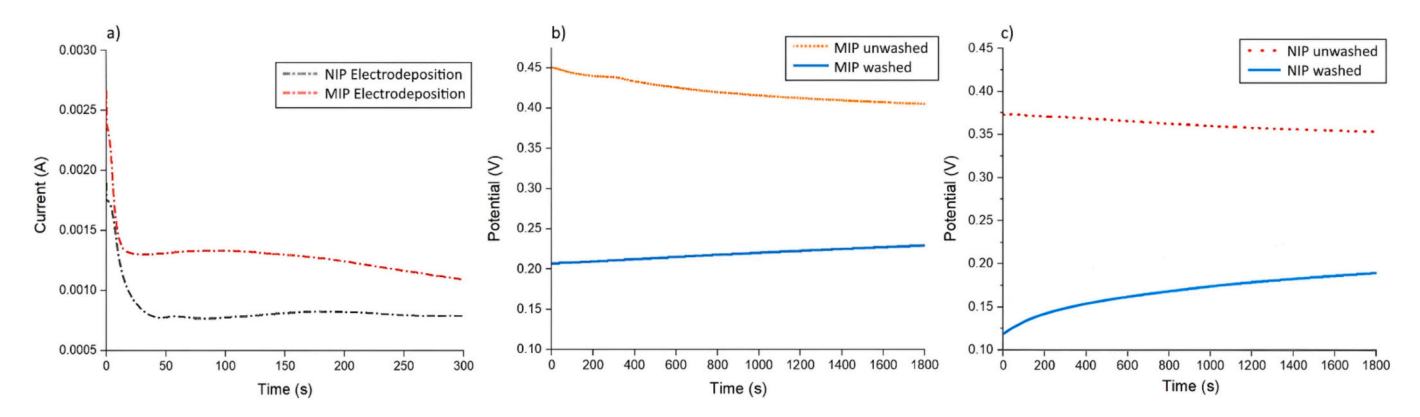
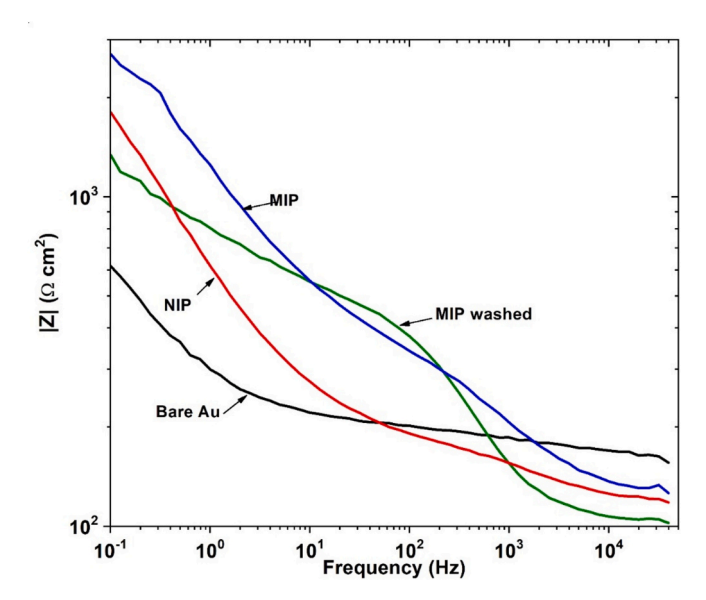


Fig. 4. a) Chronoamperometry electrodeposition of polypyrrole-DSA for MIP and NIP, b) MIP electrode OCP response in KCl  $0.1 \text{ mol} \cdot L^{-1}$  before (red) and after (blue) been washed with NaOH to elude the template c) NIP electrode OCP response in KCl  $0.1 \text{ mol} \cdot L^{-1}$ . M before (red) and after (blue) been washed with NaOH. (For interpretation of the references to colour in this figure legend, the reader is referred to the web version of this article.)



**Fig. 5.** EIS Bode diagrams obtained for bare substrate, NIP electrode and MIP electrodes before and after washing in the presence of 5 mM of [Fe (CN)<sub>6</sub>] $^{3-/4-}$  as redox probe.

lactose blocked the sites available for the probe to access the electrode surface. After washing of the MIP electrode and the consequent formation of the imprinted cavities, the impedance module in low-frequency region (curve d) remarkably decreased from 2721  $\Omega \cdot \text{cm}^2$  to 1344  $\Omega \cdot \text{cm}^2$  at 0.1 Hz, indicating that the cavities formed in the polymeric structure allowed  $\frac{1}{8}$  better electron transfer  $\frac{1}{8}$  at the electrode surface. These EIS results agree with the literature [60] and confirm the presence of imprinted cavities for lactose recognition in the polymeric structure.

#### 3.3. Selectivity of MIPs and NIPs electrode response to lactose

Once the changes undergone by the sensor after the electropolymerisation of the MIP and NIP have been characterized, it is crucial to ensure that significant differences exist in their responses in the presence of the target molecule, lactose. To achieve this, measurements will be conducted at increasing concentrations of lactose. For this study, both sensors (MIP and NIP) are immersed in a solution where incremental additions of lactose are made, and their OCP responses are measured in 0.1  $\rm mol\cdot L^{-1}$  KCl (Fig. 6).

To ensure signal reliability, all open circuit potential (OCP) values in this study were recorded after 1800 s of immersion, when the sensor signal had reached a stable plateau. Under these steady-state conditions, the coefficient of variation for the NIP sensor at the lowest lactose concentration was 1.03 %, while for the MIP sensor it was 2.68 %, confirming good reproducibility and minimal signal drift at the

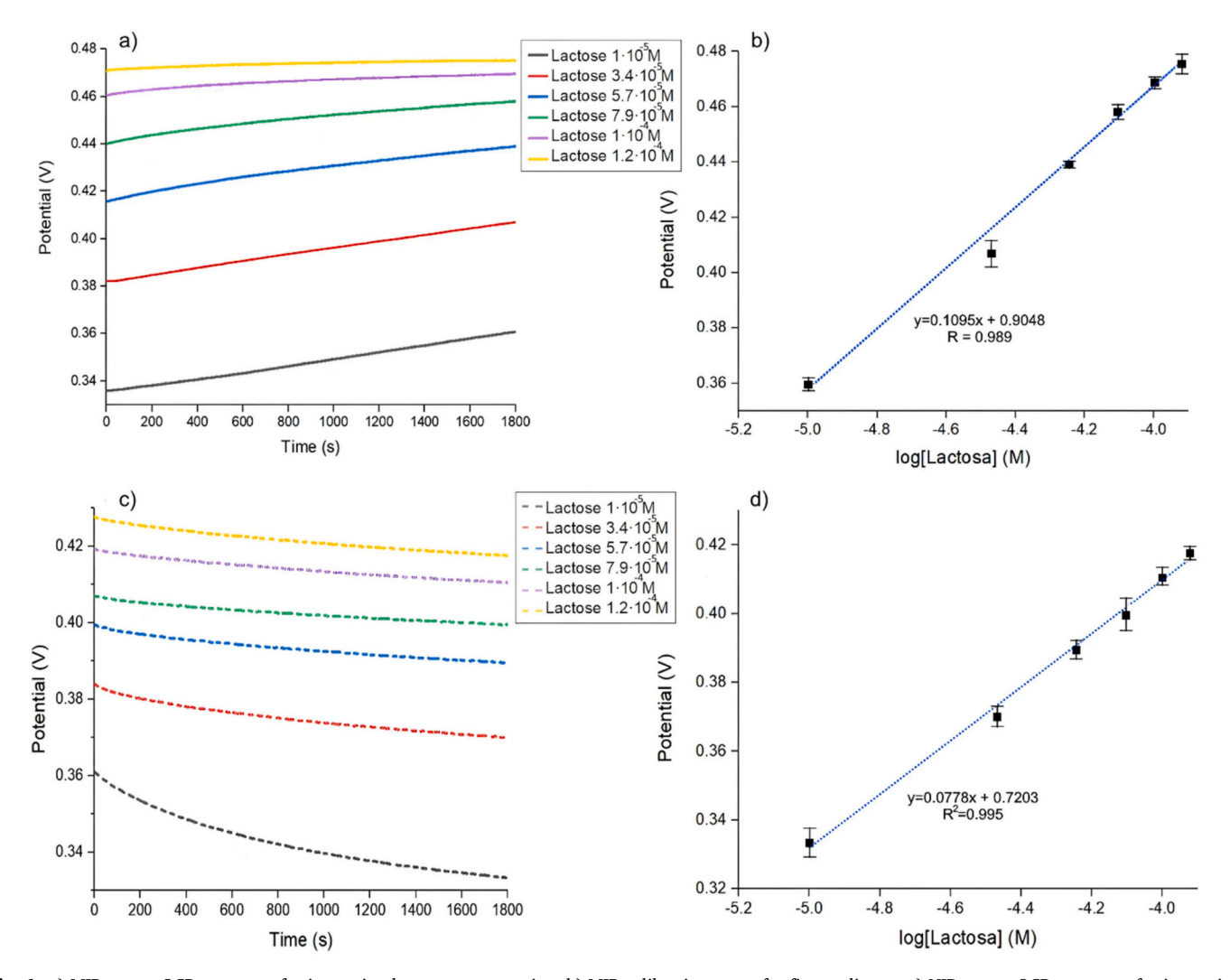


Fig. 6. a) MIP sensor OCP responses for increasing lactose concentration, b) MIP calibration curve for five replicates, c) NIP sensor OCP responses for increasing lactose concentration, d) NIP calibration curve e for five replicates.

#### measurement point.

In Fig. 6a and c, the plots depict an example of the OCP potential vs. time for increasing lactose concentrations, ranging from  $1\times 10^{-5}$  mol·L $^{-1}$  to  $1.2\times 10^{-4}$  mol·L $^{-1}$ . For the MIP sensor (Fig. 6a), the potential increases with higher lactose concentrations with significant differences between the potential curves for different concentrations, been the highest potential observed at  $1.2\times 10^{-4} \text{mol·L}^{-1}$ . The increase in OCP values with increasing lactose content can be explained by the varying affinity of the imprinted cavities. When lactose content is low, the lactose molecules occupy the high-affinity imprinted sites on the MIP electrode surface. As the lactose content increases, the lactose molecules also occupy low-affinity sites deeper within the polymeric membrane, causing an increase in membrane potential measured in OCP tests. For this reason, this result suggests the effectiveness of the MIP sensor in detecting lactose.

On the other hand, the NIP sensor (Fig. 6c) shows a similar trend of increasing potential over time for each concentration, but the overall potential values are lower. The separation between the curves is less pronounced, indicating lower sensitivity compared to the MIP. The superior performance of the MIP sensors is likely due to the specific recognition sites for lactose, which are absent in the NIP sensor. This conclusion is consistent with several studies in which polypyrrole-based electrochemical sensors have been developed, with a reduced selectivity and sensitivity nevertheless capable to detect changes in sample composition [69,70].

The potentiometric response of the MIP sensor is attributed to the selective interaction between lactose molecules and the imprinted cavities formed during the electropolymerization of polypyrrole in the presence of lactose, followed by template removal using NaOH. These cavities are likely to possess a size, shape, and functional group orientation complementary to the lactose molecule, allowing for selective rebinding. The recognition process is mainly driven by hydrogen bonding between the hydroxyl groups of lactose and polar functional groups in the polypyrrole matrix, as well as dipole-dipole interactions, which have been reported as dominant forces in MIP-analyte recognition [68,71,72]. Upon immersion of the sensor in a lactose-containing solution, these recognition sites become reoccupied by lactose molecules, as if the matrix "remembers" the templating lactose. This rebinding alters the local electrostatic environment at the polymer/ electrolyte interface, inducing a redistribution of surface charges and reorganizing the electrical double layer. As a result, the potential measured at open circuit shifts significantly. The observed increase in OCP with rising lactose concentration can be attributed to the accumulation of bound analyte molecules, which modify the ionic strength and potential drop across the Stern layer of the double layer, in line with previous studies on potentiometric MIP sensors [22,73,74]. This mechanism accounts for the higher sensitivity and specificity observed in the MIP sensor compared to the NIP, which lacks such selective binding sites. The OCP shift thus reflects the molecular recognition event at the electrode surface.

Fig. 6b and d present the calibration curves for the MIP and NIP sensors, respectively, plotting potential against lactose concentration. Both sensors demonstrated a strong linear relationship, with the correlation coefficients ( $R^2$ ) being 0.989 for the MIP sensor and 0.995 for the NIP sensor. However, the MIP sensor exhibits higher potential values and a steeper slope in the calibration curve of 0.1095, reflecting greater sensitivity to lactose. The NIP sensor, while showing a strong linear correlation, has lower potential values and a less steep slope, with a value of 0.0778, indicating reduced sensitivity as previously reported in this work. This behaviour of the NIP has been previously reported in previous studies of molecular imprinted sensors [75–77].

Moreover, the detection limits (LOD) of both MIP and NIP sensors were calculated based on their calibration curves. The MIP sensor exhibited a LOD of  $4.16\cdot10^{-5}~\text{mol}\cdot\text{L}^{-1},$  while the NIP sensor showed a LOD of  $6.09\cdot10^{-5}~\text{mol}\cdot\text{L}^{-1}.$  These results shows that there is a slight increase in the sensitivity of the MIP sensor compared to the NIP, which

can be attributed to the specific affinity of its imprinted cavities for lactose molecules. Both LODs present values similar to those obtained in previous works on polypyrrole sensors [78,79], with those obtained with the MIP being slightly higher thanks to the creation of specific cavities. This differential performance not only underscores the importance of molecular imprinting in achieving high sensitivity and specificity, highlighting its potential for practical applications but further support that the specific rebinding of lactose in imprinted cavities plays a dominant role in the observed potentiometric response.

In conclusion, the MIP-based potentiometric sensor as it was expected has better performance than the NIP, as demonstrated by higher sensitivity and more pronounced potential changes with increasing lactose concentrations. In addition, the potentiometric performance of the MIP sensor developed in this study was compared with other sensors reported in the literature (Table 2). Notably, although the limit of detection (LOD) of the MIP sensor is slightly higher than some enzymatic sensors, it remains within the same order of magnitude. Furthermore, the straightforward fabrication process of the MIP sensor offers a significant advantage over enzymatic sensors, which often require complex immobilization procedures and are susceptible to environmental conditions.

# 3.4. Effect of various potential interferents

To study the selectivity of the MIP sensor, an interference test was conducted using sugars commonly found in milk. The selected sugars were galactose and glucose, which are prevalent in dairy products and could potentially interfere with lactose detection.

Fig. 7. shows the results of the OCP values of the MIP sensor for increasing concentrations of (a) galactose and (b) glucose, respectively. In both cases, unlike the case with lactose, the potential measurements for galactose and glucose do not show a clear trend correlating with the concentrations. This lack of order in the potentiometric response indicates that the MIP sensor does not have a high affinity or specificity for either of these sugars. Despite having a structural similarity to lactose, glucose and galactose do not perfectly fit, into the imprinted cavities made especially for lactose, which results in the observed non-linearity. The binding affinity and interaction dynamics differ, leading to variable and inconsistent changes in the performance of sensor. This behaviour further supports the notion that the molecularly imprinted polymer is highly specific to lactose and does not exhibit significant cross-reactivity with other sugars commonly present in milk. The specificity of the MIP sensor towards lactose is crucial for its application in complex matrices like milk, where various sugars are present, ensuring accurate and selective detection of lactose without interference from other similar compounds.

Beyond glucose and galactose, which were explicitly chosen due to their structural similarity to lactose, other milk components such as proteins and fats could potentially act as interferents in complex

Sensing of lactose using proposed MIP sensor and other reports.

0 0	1 1		
Sensor	Linear range	LOD	References
CDH/AuNPs/graphite (enzymatic)	$10~\mu M - 300~\mu M$	3.5 μΜ	[80]
PPy-DBSb electrode (enzymatic)	0.3 mM - 1.22 mM	2 μΜ	[81]
APPIBr/CDH/GCE (enzymatic)	$50~\mu M - 3~mM$	0.58 μΜ	[82]
Cu foam (non-enzymatic)	0.18 mM – 3.47 mM	9.30 μΜ	[83]
MIP sensor (non-enzymatic)	$10~\mu M-120~\mu M$	41.6 μΜ	This work

CDH: Cellobiose dehydrogenase; AuNPs: gold nanoparticles; PPy: polypyrrole; DBS: dodecylbenzenesulfonate; APPIBr: 3-Amine-N-[3-(Npyrrole)propyl]imidazole bromide; GCE: glassy carbon electrode.

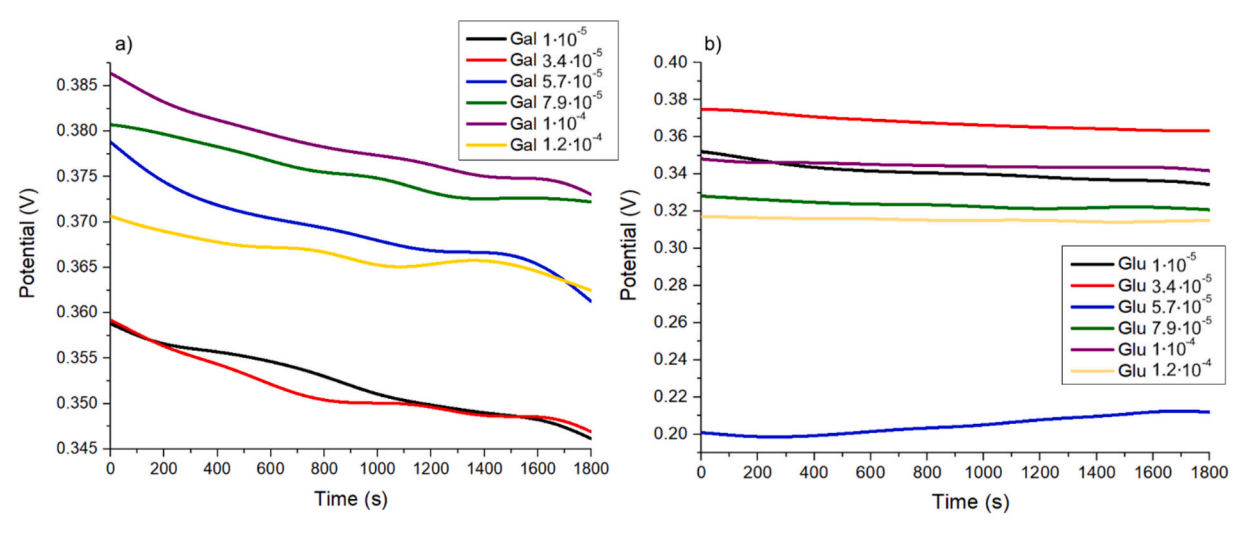


Fig. 7. Signals obtained from the MIP sensor for increasing concentrations of (a) galactose and (b) glucose.

matrices. However, due to the size-exclusion mechanism and the high molecular specificity of the imprinted cavities, these macromolecules are unlikely to penetrate or interact with the recognition sites. This property, combined with the electrochemical nature of the detection process, helps to minimize nonspecific interactions, as previously reported in MIP-based sensors used in biological and food samples [84,85].

# 3.5. Response time, reversibility and life-time of sensors

Before applying the developed sensor for lactose detection in real samples, it is essential to verify their shelf life and recovery over time. This evaluation ensures that the sensors maintain consistent performance and can be reused effectively.

After measuring lactose, the sensors were immersed in a 0.1 M NaOH solution to elute the molecules from the cavities. To determine the effectiveness of the process, the potential variation in the OCP signals for the MIP and the NIP have been analysed after the eluting phase between lactose samples. In both cases, the potential varied by a maximum of 0.02 V between subsequent measurements, indicating variations that are less than 7 % of the coefficient of variation. This result is below the highest variation coefficient (10.5 % variance) noted in the detection of increasing lactose concentrations, indicating good sensor recovery.

The combined results from both parts indicate that the slight increases in potential observed for the MIP (Fig. 8a) and NIP (Fig. 8b) sensors are not substantial enough to have a significant impact in their reusability for at least the four measurements performed. Notably, the MIP sensor exhibited more consistent recovery with a lower variation coefficient (5.7 %) compared to the NIP sensor (6.6 %). This finding underscores the stability and reliability of the MIP sensor for repeated measurements, confirming its suitability for practical applications in lactose detection.

# 3.6. Practical application in analysis of cow milks

After characterizing the MIP and NIP electrodes, they were immersed in milk samples with varying lactose content to evaluate their analytical performance. The sensors were immersed in the samples under stirring for 30 min, and then the OCP was measured in KCl. Fig. 9 shows the OCP responses of the electrodes in milk samples. As observed, the higher the lactose content, the higher the potential response of both MIP and NIP sensors. However, Fig. 9a demonstrates that the MIP electrodes could better distinguish between milk samples with medium and high lactose content compared to NIP electrodes (Fig. 9.b). This result indicates that the imprinted cavities on the polymeric surface are occupied by lactose molecules, making MIP electrodes good candidates for quantitative

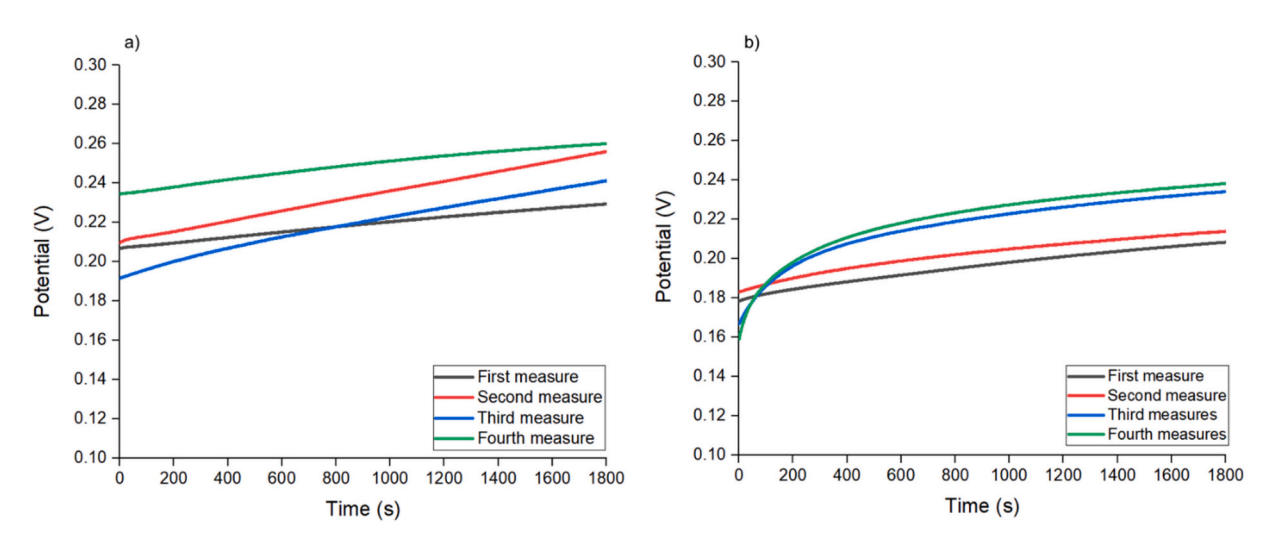


Fig. 8. a) OCP responses in  $0.1 \text{ mol} \cdot L^{-1}$ KCl of the MIP after four different measurements and b) OCP responses in  $0.1 \text{ mol} \cdot L^{-1}$ KCl of the NIP after four different measurements.

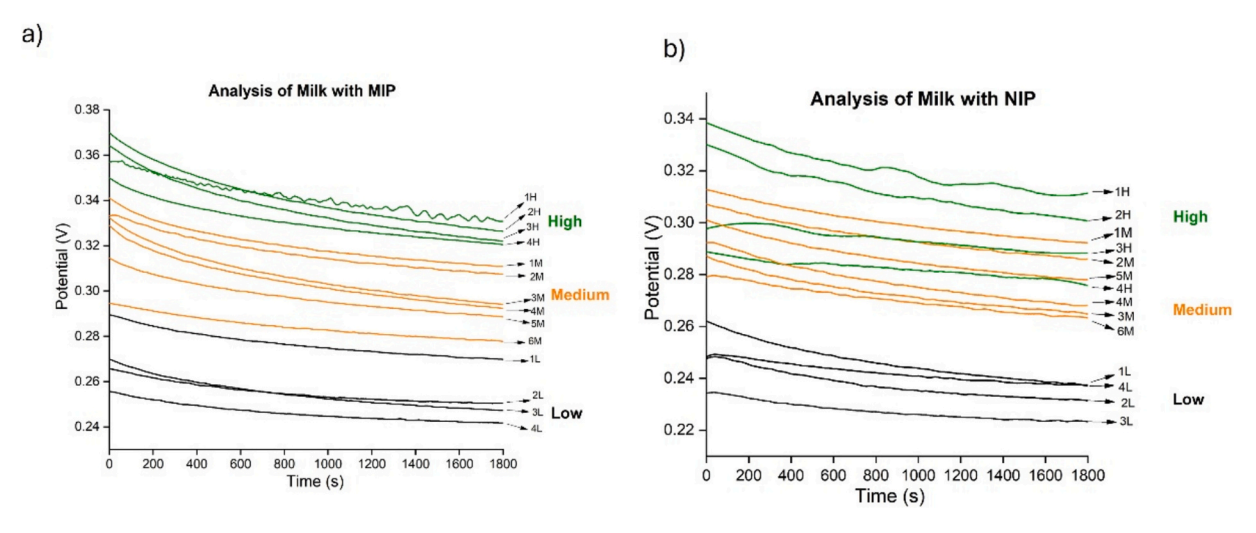


Fig. 9. Open circuit potential responses of (a) MIP and (b) NIP electrodes in milk samples with different lactose content.

analysis of lactose in cow milk samples.

The OCP responses for NIP electrodes were less efficient in analysing milk with different lactose contents, even though low lactose content milk was well differentiated from high/medium lactose milk content, this confirms the importance of the imprinted templating process in enhancing electrode performance towards the target molecule. These results have been observed previously [60].

For NIP electrodes, a similar sequence was observed: as lactose content increased, the OCP value also increased. In this case, the changes in OCP values can be attributed to the placement of lactose molecules in cavities formed by the inherent roughness of the polymeric membrane, rather than the presence of imprinted cavities.

#### 3.7. Statistical analysis

The electroanalytical capacity of the MIP and NIP electrodes to discriminate cow milk samples with different lactose content was evaluated using Principal Component Analysis (PCA). This analysis identifies the best discriminating components without any prior knowledge of groups, as it is an unsupervised method, preventing any prior classification of the data. For this purpose, the OCP values at different times of each cow milk sample were used as the input data source for statistical analysis. Fig. 10 shows the PCA score plots of the responses obtained with MIP and NIP electrodes towards cow milks. In both cases, PC1 and

PC2 explained more than the 95 % of the total covariance of the data, however it can be seen that the capability of discrimination is much better when using MIP electrodes, since the cow milks were separately located depending on the lactose content confirming the good performance of the imprinted electrode.

The OCP responses provided by the MIP and NIP electrodes have been correlated with the lactose content of the analysed cow milk samples using Partial Least Squares regression (PLS-1). The regression models were performed using the full cross-validation function as an internal validation technique for the mathematical model. In this analysis, calibration fits the model to the available data, while validation checks the model with new data. The OCP values obtained with the electrodes for cow milk samples were used as the matrix of predictors

**Table 3**Results of Partial Least Squares regressions models (PLS-1) correlating the OCP values of the MIP and NIP electrodes with the lactose content.

MIP electrode	$R_C^2$ (a)	RMSE <sub>C</sub> (b)	$R_P^2$ (c)	$RMSE_{P}(d)$	Factors
	0.9462	0.1420	0.9186	0.1881	2
NIP electrode	$R_C^2$ (a)	$RMSE_C$ (b)	$R_P^2$ (c)	$RMSE_{P}(d)$	Factors
	0.8505	0.2368	0.7483	0.3308	2

- (a), (c) Squared correlation coefficients in calibration and prediction.
- (b), (d) Root mean square errors in calibration and prediction.

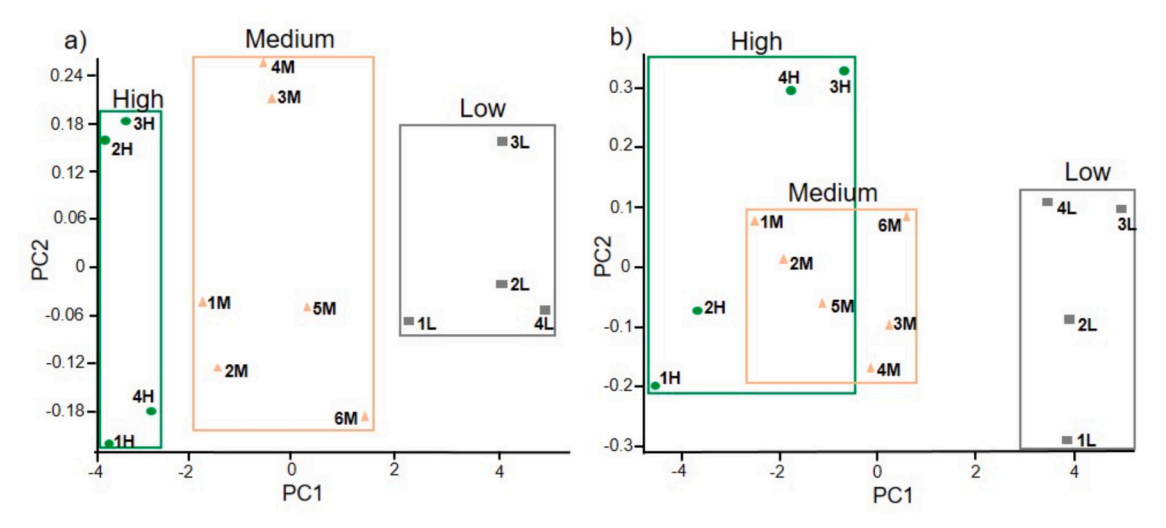


Fig. 10. Scores plots corresponding to the PCA analysis of cow milks using (a) MIP and (b) NIP electrodes, respectively.

(X), while the lactose content values were established as the matrix of expected responses (Y). Table 3 presents the statistical results obtained from the PLS-1 analysis using 2 factors. In the case of the MIP electrode, the higher values of  $\mathbb{R}^2$  and the lower errors (in both calibration and prediction) show the great effectiveness of the model in calibrating and validating the model. On the other hand, the NIP electrode has evidenced lower  $\mathbb{R}^2$  values with higher errors than those attributed to MIP electrodes, confirming once again a clear disadvantage compared to imprinted electrodes.

Finally, the analytical performance of the sensors was used to predict the lactose content from the OCP values obtained in cow milk samples using Support Vector Machine Regression (SVMR). The SVMR models were created using the following parameters: SVM type: Regression (epsilon SVR), Kernel type: Linear, C value: 1, Weights: All 1.0, and Cross-validation segment size: 10. After constructing the SVMR model, the regression models were used to predict the lactose content of 5 cow milk samples that were not included in the creation of the models. The results, shown in Table 4, are compared with the experimental results obtained by HPLC. As observed, the predicted lactose content values were close to those obtained by HPLC. Generally, the relative errors were lower using MIP than NIP for sensors predicting lactose content. Moreover, MIP sensors demonstrated better prediction capability for cow milk with high and medium lactose content.

# 4. Conclusions

This work presents a study of polypyrrole-based MIP potentiometric sensors for analysing lactose content in milk. The performance of the MIP sensor is compared to that of the corresponding polypyrrole-based NIP electrode to demonstrate the advantage of the imprinted cavities created in MIP electrodes by removing the lactose template molecule from the polymeric structure. The formation of cavities for lactose recognition was corroborated by different analysis including Raman spectroscopy, SEM, AFM and EIS. Regarding the electrodeposition method, chronoamperometry results demonstrated that the increase in current intensity during MIP electrodeposition, compared to NIP, is due to the presence of lactose molecules during polymerization that enhances the conductivity of the polypyrrole facilitating the formation of specific cavities. The OCP values observed for the MIP and NIP sensors were higher before washing the electrodes and decreased after they were washed with NaOH. However, the potentials for the NIP sensor were lower than those obtained with the MIP, suggesting that the MIP has a more organized and higher-energy surface state due to these specific cavities. The sensor responses to different lactose concentrations showed that the OCP values increased with increasing lactose content, although the NIP sensor showed lower OCP values and sensitivity than the MIP sensor. This result was confirmed by measuring milk samples with different lactose content: the NIP electrode was less capable of distinguishing between medium and high lactose content, likely due to the lack of specific cavities for lactose recognition. The response of MIP sensor to different interfering sugars demonstrated that increasing concentrations of them did not show a correlation to concentration, indicating that the MIP sensor does not have affinity for these sugars. Finally, statistical analyses demonstrated that the MIP electrode was superior in discriminating milk samples with different lactose content and produced better PLS-1 regression models with higher correlation coefficients and lower errors. Using SVMR, it was possible to predict the lactose content in milk, based on data provided by the MIP and NIP electrodes, although the MIP electrode generally showed lower relative errors in prediction. Moreover, although the differences in sensitivity and detection limit between the MIP and NIP sensors are modest (LOD of  $4.16 \cdot 10^{-5} \text{ mol} \cdot \text{L}^{-1}$  for MIP vs.  $6.09 \cdot 10^{-5} \text{ mol} \cdot \text{L}^{-1}$  for NIP), the key advantage of the MIP sensor lies in its higher selectivity and specificity for lactose recognition, as evidenced in several aspects of this study. First, the OCP response of the MIP sensor shows a clearer and more consistent trend with increasing lactose concentrations, with a higher calibration slope (0.1095 vs. 0.0778) and better separation of potential values. This reflects a more structured and selective interaction with lactose. Second, interference studies demonstrated that the MIP sensor exhibits negligible response to structurally similar sugars like glucose and galactose, whereas NIP sensors can still show non-specific adsorption due to their rough morphology. This selective behaviour is crucial for practical applications in complex food matrices such as milk. Third, multivariate analyses including PCA, PLS-1 and SVM regression highlight that the MIP sensor achieves better sample discrimination and more accurate lactose prediction, with lower prediction errors compared to the NIP sensor (RMSEP of 0.1881 for MIP vs. 0.3308 for NIP in PLS-1 models). In conclusion, although the MIP sensor shows only moderate numerical improvements in sensitivity and LOD, its superior selectivity, reproducibility, and performance in real milk samples confirm the significant role of molecular imprinting in lactose-specific detection. Finally, the MIP sensor demonstrated consistent and reliable performance over multiple measurements, with minimal potential drift and a lower variation coefficient compared to the NIP sensor. This result is of great interest to the food industry and has advantages over existing methods, as it opens up the possibility of predicting lactose content with simple and easy measurements. However, before such sensors can be successfully commercialised, it would be desirable to improve the affinity of the polymers for the target molecule (using different polymers), to improve the ratio between specific and non-specific binding and to develop more efficient immobilization protocols.

# CRediT authorship contribution statement

C. Perez-Gonzalez: Writing – original draft, Methodology, Investigation, Data curation. C. Garcia-Hernandez: Writing – original draft, Methodology, Investigation, Data curation, Conceptualization. C. Garcia-Cabezon: Writing – original draft, Project administration, Investigation, Funding acquisition, Conceptualization. M.L. Rodriguez-Mendez: Writing – original draft, Project administration, Investigation, Funding acquisition, Conceptualization. F. Martin-Pedrosa: Writing – original draft, Software, Investigation, Data curation, Conceptualization.

# Declaration of competing interest

The authors declare the following financial interests/personal relationships which may be considered as potential competing interests:

Table 4
Lactose content predicted in milk samples with regression models performed by SVM.

Milk sample	Lactose content obtained by HPLC	MIP electrodes		NIP electrodes	
		Lactose content predicted	Relative error  %	Lactose content predicted	Relative error  %
1H* (1426)	5.48	5.32	2.92	5.53	0.91
3H* (1446)	5.29	5.25	0.76	4.85	8.32
5 M* (1503)	4.66	4.70	0.86	4.94	6.01
1 L* (963)	4.03	4.39	8.93	4.23	4.96
4 L* (1135)	3.37	3.95	17.21	4.14	22.85

Cristina Garcia-Cabezon reports financial support was provided by Spain Ministry of Science and Innovation. Maria Luz Rodriguez Mendez reports financial support was provided by Junta de Castilla y León Consejería de Educación. If there are other authors, they declare that they have no known competing financial interests or personal relationships that could have appeared to influence the work reported in this paper.

#### Acknowledgments

This work was supported by Ministerio de Ciencia Innovacion y Universidades -FEDER Plan Estatal (*PID2021-1223650B-100*). Junta de Castilla y Leon- FEDER VA117P24 and CLU-2019-04 BIOECOUVA Unit of Excellence, and Plan Tractor En Materiales Avanzados Enfocado A Los Sectores Industriales Claves En Castilla Y León: Agroalimentario, Transporte, Energía Y Construcción (MA2TEC). C. Pérez-González has been financed with the call for UVa 2020 predoctoral contracts, cofinanced by Banco Santander.

# Data availability

Data will be made available on request.

#### References

- G. Czyżak-Runowska, et al., Lactose content and selected quality parameters of sheep Milk fermented beverages during storage, Animals 12 (22) (2022), https://doi.org/10.3390/ani12223105.
- [2] A. Shaukat, et al., Systematic Review: Effective Management Strategies for Lactose Intolerance [Online]. Available, www.annals.org.
- [3] A.M. Prentice, Dairy products in global public health, Am. J. Clin. Nutr. 99 (5) (2014), https://doi.org/10.3945/ajcn.113.073437.
- [4] K.A. Hettinga, "Lactose in the dairy production chain," in Lactose: Evolutionary Role, Health Effects, and Applications, Elsevier, 2019, pp. 231–266, https://doi.org/ 10.1016/B978-0-12-811720-0.00006-4.
- [5] M. Pokrzywnicka, R. Koncki, Disaccharides Determination: A Review of Analytical Methods, Taylor and Francis Ltd. (2018), https://doi.org/10.1080/ 10408347.2017.1391683.
- [6] P.S. Rao, P. Singh, V. Sharma, S. Arora, Traditional analytical approaches for lactose residues determination in lactose hydrolysed milks: A review, Academic Press. (2021), https://doi.org/10.1016/j.lwt.2021.112069.
- [7] D.C.S.Z. Ribeiro, et al., Determination of the lactose content in low-lactose milk using Fourier-transform infrared spectroscopy (FTIR) and convolutional neural network, Heliyon 9 (1) (2023), https://doi.org/10.1016/j.heliyon.2023.e12898.
- [8] D.W. Kimmel, G. Leblanc, M.E. Meschievitz, D.E. Cliffel, Electrochemical sensors and biosensors, Anal. Chem. 17 (2012), https://doi.org/10.1021/ac202878q.
- [9] J. Baranwal, B. Barse, G. Gatto, G. Broncova, A. Kumar, Electrochemical Sensors and Their Applications: A Review, MDPI, 2022, https://doi.org/10.3390/ chemosensors10090363.
- [10] Ö. Isildak, O. Özbek, Application of Potentiometric Sensors in Real Samples, Taylor and Francis Ltd., 2021, https://doi.org/10.1080/10408347.2019.1711013.
- [11] E. Zdrachek, E. Bakker, Potentiometric Sensing, Am. Chem. Soc. (2021), https://doi.org/10.1021/acs.analchem.0c04249.
- [12] C. Pérez-González, et al., Analysis of Milk using a portable potentiometric electronic tongue based on five polymeric membrane sensors, Front. Chem. 9 (2021), https://doi.org/10.3389/fchem.2021.706460.
- [13] C. Perez-Gonzalez, C. Garcia-Hernandez, C. Garcia-Cabezon, M.L. Rodriguez-Mendez, L. Dias, F. Martin-Pedrosa, Analysis of milk adulteration by means of a potentiometric electronic tongue, J. Dairy Sci. (2024), https://doi.org/10.3168/ ids. 2024.25140
- [14] S. Bayrak, H. Gergeroglu, Graphene-based biosensors in milk analysis: A review of recent developments, Elsevier Ltd. (2024), https://doi.org/10.1016/j. foodchem.2023.138257.
- [15] C. Perez-Gonzalez, C. Salvo-Comino, F. Martin-Pedrosa, M.L. Rodriguez-Mendez, C. Garcia-Cabezon, A new data analysis approach for an AgNPs-modified impedimetric bioelectronic tongue for dairy analysis, Food Control 156 (2024), https://doi.org/10.1016/j.foodcont.2023.110136.
- [16] Q. Chen, M. Meng, W. Li, Y. Xiong, Y. Fang, Q. Lin, Emerging biosensors to detect aflatoxin M1 in milk and dairy products, Elsevier Ltd. (2022), https://doi.org/ 10.1016/j.foodchem.2022.133848.
- [17] M.A. Farag, M. Tanios, S. AlKarimy, H. Ibrahim, H.A. Guirguis, Biosensing Approaches to Detect Potential Milk Contaminants: A Comprehensive Review, Taylor and Francis Ltd., 2021, https://doi.org/10.1080/19440049.2021.1914864.
- [18] G. Murugaboopathi, V. Parthasarathy, C. Chellaram, T.P. Anand, S. Vinurajkumar, Applications of biosensors in food industry, Biosci. Biotechnol. Res. Asia (2013), https://doi.org/10.13005/bbra/1185.
- [19] Haupt Karsten, V. Linares Ana, Bompart Marc, Tse Sum Bu Bernadette, Molecular Imprinting 325, Topics in Current Chemistry, 2012.

- [20] M. Dabrowski, P. Lach, M. Cieplak, W. Kutner, Nanostructured molecularly imprinted polymers for protein chemosensing, Elsevier Ltd. (2018), https://doi. org/10.1016/j.bios.2017.10.045.
- [21] E. Turiel, A. Martín-Esteban, Molecularly Imprinted Polymers for Sample Preparation: A Review, Anal. Chim. Acta (2010), https://doi.org/10.1016/j. aca.2010.04.019.
- [22] R.N. Liang, D.A. Song, R.M. Zhang, W. Qin, Potentiometrie sensing of neutral species based on a uniform-sized molecularly imprinted polymer as a receptor, Angew. Chem. Int. Ed. 49 (14) (2010) 2556–2559, https://doi.org/10.1002/ anic 200906720
- [23] J. Ashley, et al., Molecularly imprinted polymers for sample preparation and biosensing in food analysis: Progress and perspectives, Biosens. Bioelectron. 91 (2017) 606–615, https://doi.org/10.1016/J.BIOS.2017.01.018.
- [24] M. Zeilinger, H. Sussitz, W. Cuypers, C. Jungmann, P. Lieberzeit, Mass-sensitive sensing of melamine in dairy products with molecularly imprinted polymers: matrix challenges, Sensors 19 (2019) 2366, https://doi.org/10.3390/S19102366.
- [25] J. Gañán, et al., Development of a molecularly imprinted polymer-matrix solid-phase dispersion method for selective determination of β-estradiol as anabolic growth promoter in goat milk, Anal. Bioanal. Chem. 403 (10) (2012) 3025–3029, https://doi.org/10.1007/S00216-012-5794-0/TABLES/2.
- [26] M.A. Tantawy, A.M. Yehia, H.T. Elbalkiny, All-solid-state chip utilizing molecular imprinted polymer for erythromycin detection in milk samples: printed circuit board-based potentiometric system, Microchim. Acta 190 (10) (2023) 1–11, https://doi.org/10.1007/S00604-023-05959-W/FIGURES/1.
- [27] A. Mortari, L. Lorenzelli, Recent sensing technologies for pathogen detection in milk: a review, Biosens. Bioelectron. 60 (2014) 8–21, https://doi.org/10.1016/J. BIOS 2014 03 063
- [28] I. Basozabal, A. Guerreiro, A. Gomez-Caballero, M. Aranzazu Goicolea, R.J. Barrio, Direct potentiometric quantification of histamine using solid-phase imprinted nanoparticles as recognition elements, Biosens. Bioelectron. 58 (2014) 138–144, https://doi.org/10.1016/J.BIOS.2014.02.054.
- [29] Y. Pan, J. Liu, J. Wang, Y. Gao, N. Ma, Invited review: application of biosensors and biomimetic sensors in dairy product testing, J. Dairy Sci. 107 (10) (2024) 7533–7548, https://doi.org/10.3168/JDS.2024-24666.
- [30] D. Saritha, et al., A simple, highly sensitive and stable electrochemical sensor for the detection of quercetin in solution, onion and honey buckwheat using zinc oxide supported on carbon nanosheet (ZnO/CNS/MCPE) modified carbon paste electrode, Electrochim. Acta 313 (2019) 523–531, https://doi.org/10.1016/J. ELECTACTA.2019.04.188.
- [31] Y. Yang, X. Shen, Preparation and Application of Molecularly Imprinted Polymers for Flavonoids: Review and Perspective, Molecules 27 (2022) 7355, https://doi. org/10.3390/MOLECULES27217355.
- [32] J. Wang, R. Liang, W. Qin, Molecularly imprinted polymer-based potentiometric sensors, TrAC Trends Anal. Chem. 130 (2020) 115980, https://doi.org/10.1016/J. TRAC.2020.115980.
- [33] R. Liang, R. Zhang, W. Qin, Potentiometric sensor based on molecularly imprinted polymer for determination of melamine in milk, Sensors Actuators B Chem. 141 (2) (2009) 544–550, https://doi.org/10.1016/j.snb.2009.05.024.
- [34] A.S. Sacramento, F.T.C. Moreira, J.L. Guerreiro, A.P. Tavares, M.G.F. Sales, Novel biomimetic composite material for potentiometric screening of acetylcholine, a neurotransmitter in Alzheimer's disease, Mater. Sci. Eng. C 79 (2017) 541–549, https://doi.org/10.1016/j.msec.2017.05.098.
- [35] A. Ghorbani, R. Ojani, M.R. Ganjali, J. Raoof, Direct voltammetric determination of carbendazim by utilizing a nanosized imprinted polymer/MWCNTs-modified electrode, J. Iran. Chem. Soc. 18 (11) (2021) 3109–3118, https://doi.org/ 10.1007/s13738-021-02255-3.
- [36] Y. Zhou, B. Yu, K. Levon, Potentiometric sensor for dipicolinic acid, Biosens. Bioelectron. 20 (9) (2005) 1851–1855, https://doi.org/10.1016/j. bios.2004.05.005.
- [37] T. Alizadeh, R.E. Sabzi, H. Alizadeh, Synthesis of nano-sized cyanide ion-imprinted polymer via non-covalent approach and its use for the fabrication of a CN-selective carbon nanotube impregnated carbon paste electrode, Talanta 147 (2016) 90–97, https://doi.org/10.1016/j.talanta.2015.09.043.
- [38] G. D'Agostino, G. Alberti, R. Biesuz, M. Pesavento, Potentiometric sensor for atrazine based on a molecular imprinted membrane, Biosens. Bioelectron. 22 (1) (2006) 145–152, https://doi.org/10.1016/j.bios.2006.05.014.
- [39] J.J. Belbruno, Molecularly Imprinted Polymers, Am. Chem. Soc. (2019), https://doi.org/10.1021/acs.chemrev.8b00171.
- [40] S. Ramanavicius, U. Samukaite-Bubniene, V. Ratautaite, M. Bechelany, A. Ramanavicius, Electrochemical molecularly imprinted polymer based sensors for pharmaceutical and biomedical applications (review), Elsevier B.V. (2022), https://doi.org/10.1016/j.jpba.2022.114739.
- [41] H. Rao, et al., A novel electrochemical sensor based on au@PANI composites film modified glassy carbon electrode binding molecular imprinting technique for the determination of melamine, Biosens. Bioelectron. 87 (2017) 1029–1035, https:// doi.org/10.1016/j.bios.2016.09.074.
- [42] A. Palma-Cando, I. Rendón-Enríquez, M. Tausch, U. Scherf, Thin functional polymer films by electropolymerization, Nanomaterials 9 (8) (2019), https://doi. org/10.3390/nano9081125.
- [43] C. Yan, X. Liu, R. Zhang, Y. Chen, G. Wang, A selective strategy for determination of ascorbic acid based on molecular imprinted copolymer of o-phenylenediamine and pyrrole, J. Electroanal. Chem. 780 (2016) 276–281, https://doi.org/10.1016/ j.jelechem.2016.09.046.
- [44] A.G. Ayankojo, J. Reut, V. Ciocan, A. Öpik, V. Syritski, Molecularly imprinted polymer-based sensor for electrochemical detection of erythromycin, Talanta 209 (2020), https://doi.org/10.1016/j.talanta.2019.120502.

[45] L.P. Liu, Z.J. Yin, Z.S. Yang, A l-cysteine sensor based on Pt nanoparticles/poly(o-aminophenol) film on glassy carbon electrode, Bioelectrochemistry 79 (1) (2010) 84–89, https://doi.org/10.1016/j.bioelechem.2009.12.003.

C. Perez-Gonzalez et al.

- [46] Z. Lu, et al., A dual-template imprinted polymer electrochemical sensor based on AuNPs and nitrogen-doped graphene oxide quantum dots coated on NiS2/biomass carbon for simultaneous determination of dopamine and chlorpromazine, Chem. Eng. J. 389 (2020), https://doi.org/10.1016/j.cej.2020.124417.
- [47] A. Ramanavicius, Y. Oztekin, A. Ramanaviciene, Electrochemical formation of polypyrrole-based layer for immunosensor design, Sensors Actuators B Chem. 197 (2014) 237–243, https://doi.org/10.1016/j.snb.2014.02.072.
- [48] R.D. Crapnell, R.J. Street, V. Ferreira-Silva, M.P. Down, M. Peeters, C.E. Banks, Electrospun nylon Fibers with integrated Polypyrrole molecularly imprinted polymers for the detection of glucose, Anal. Chem. 93 (39) (2021) 13235–13241, https://doi.org/10.1021/acs.analchem.1c02472.
- [49] G. Bagdžiūnas, Theoretical design of molecularly imprinted polymers based on polyaniline and polypyrrole for detection of tryptophan, Mol Syst Des Eng 5 (9) (2020) 1504–1512. https://doi.org/10.1039/d0me00089b.
- [50] J. Agrisuelas, et al., Evaluation of the electrochemical anion recognition of NO3imprinted poly(Azure A) in NO3-/Cl3- Mixed solutions by ac-electrogravimetry, Electrochim. Acta 194 (2016) 292–303, https://doi.org/10.1016/j. electrochim. 2016.0366
- [51] H. Hikmat, Aprilia Nur Tasfiyati, Synthesis and characterization of a Polypyrrole-based molecularly imprinted polymer electrochemical sensor for the selective detection of phosphate ion, J. Anal. Chem. 78 (1) (2023) 117–124, https://doi.org/10.1134/S1061934893010057
- [52] E. Brazys, et al., Molecularly imprinted polypyrrole-based electrochemical melamine sensors, Microchem. J. 199 (2024), https://doi.org/10.1016/j. microc.2024.109890.
- [53] Z. Zhang et al., "Facile construction of a molecularly imprinted polymer-based electrochemical sensor for the detection of milk amyloid A" Mikrochim Acta, doi: https://doi.org/10.1007/s00604-020-04619-7/Published.
- [54] D. İşık, S. Şahin, M.O. Caglayan, Z. Üstündağ, Electrochemical impedimetric detection of kanamycin using molecular imprinting for food safety, Microchem. J. 160 (2021), https://doi.org/10.1016/j.microc.2020.105713.
- [55] S. Basak, R. Venkatram, R.S. Singhal, Recent advances in the application of molecularly imprinted polymers (MIPs) in food analysis, Food Control (2022), https://doi.org/10.1016/j.foodcont.2022.109074. Elsevier Ltd.
- [56] J. Ashley, et al., Synthesis of molecularly imprinted polymer nanoparticles for α-casein detection using surface plasmon resonance as a Milk allergen sensor, ACS Sens 3 (2) (2018) 418–424, https://doi.org/10.1021/acssensors.7b00850.
- [57] J.G. Pacheco, M. Castro, S. Machado, M.F. Barroso, H.P.A. Nouws, C. Delerue-Matos, Molecularly imprinted electrochemical sensor for ochratoxin a detection in food samples, Sensors Actuators B Chem. 215 (2015) 107–112, https://doi.org/ 10.1016/j.snb.2015.03.046.
- [58] C. Garcia-Hernandez, C. Garcia-Cabezon, F. Martin-Pedrosa, M.L. Rodriguez-Mendez, Analysis of musts and wines by means of a bio-electronic tongue based on tyrosinase and glucose oxidase using polypyrrole/gold nanoparticles as the electron mediator, Food Chem. 289 (2019), https://doi.org/10.1016/j. foodchem.2019.03.107.
- [59] C. Garcia-Hernandez, C. Garcia-Cabezon, F. Martin-Pedrosa, M.L. Rodriguez-Mendez, Analysis of musts and wines by means of a bio-electronic tongue based on tyrosinase and glucose oxidase using polypyrrole/gold nanoparticles as the electron mediator, Food Chem. 289 (2019) 751–756, https://doi.org/10.1016/J. FOODCHEM.2019.03.107.
- [60] J.L. da Silva, et al., Non-enzymatic lactose molecularly imprinted sensor based on disposable graphite paper electrode, Anal. Chim. Acta 1143 (2021) 53–64, https://doi.org/10.1016/j.aca.2020.11.030.
- [61] N.A. Abdallah, H.F. Ibrahim, Potentiometric sensor of graphene oxide decorated with silver nanoparticles/molecularly imprinted polymer for determination of gabapentin, Carbon Lett. 27 (2018) 50–63. Accessed: May 21, 2025. [Online]. Available: https://www.dbpia.co.kr/journal/articleDetail?nodeId=NOD E10242351.
- [62] B.M. Murphy, S.W. Prescott, I. Larson, Measurement of lactose crystallinity using Raman spectroscopy, J. Pharm. Biomed. Anal. 38 (1) (2005) 186–190, https://doi. org/10.1016/j.jpba.2004.12.013.
- [63] G.P. González, P.F. Hernando, J.S.D. Alegría, A morphological study of molecularly imprinted polymers using the scanning electron microscope, Anal. Chim. Acta (2006) 179–183, https://doi.org/10.1016/j.aca.2005.10.034.
- [64] G.P. González, P.F. Hernando, J.S.D. Alegría, A morphological study of molecularly imprinted polymers using the scanning electron microscope, Anal. Chim. Acta (2006) 179–183, https://doi.org/10.1016/j.aca.2005.10.034.
- [65] O.W. Ngwanya, M. Ward, P.G.L. Baker, Molecularly imprinted polypyrrole sensors for the detection of pyrene in aqueous solutions, Original Research (2025), https:// doi.org/10.1007/s12678-020-00638-3/Published.
- [66] B. Feier, A. Blidar, A. Pusta, P. Carciuc, C. Cristea, Electrochemical sensor based on molecularly imprinted polymer for the detection of cefalexin, Biosensors (Basel) 9 (1) (2019), https://doi.org/10.3390/bios9010031.
- [67] T. Beduk, A. Ait Lahcen, N. Tashkandi, K.N. Salama, One-step electrosynthesized molecularly imprinted polymer on laser scribed graphene bisphenol a sensor, Sensors Actuators B Chem. 314 (2020), https://doi.org/10.1016/j. snb.2020.128026.

- [68] C. Malitesta, E. Mazzotta, R.A. Picca, A. Poma, I. Chianella, S.A. Piletsky, MIP Sensors - the Electrochemical Approach, 2012, https://doi.org/10.1007/s00216-011-5405-5
- [69] X. Zheng, et al., Polypyrrole composite film for highly sensitive and selective electrochemical determination sensors, Electrochim. Acta 130 (2014) 187–193, https://doi.org/10.1016/j.electacta.2014.03.018.
- [70] K. Maksymiuk, Chemical Reactivity of Polypyrrole and its Relevance to Polypyrrole Based Electrochemical Sensors, Wiley-VCH Verlag, 2006, https://doi.org/ 10.1002/elan.200603573.
- [71] Y. Saylan, S. Akgönüllü, H. Yavuz, S. Ünal, A. Denizli, Molecularly Imprinted Polymer Based Sensors for Medical Applications, Sensors 19 (2019) 1279, https://doi.org/10.3390/S19061279.
- [72] M.P. Tiwari, A. Prasad, Molecularly imprinted polymer based enantioselective sensing devices: a review, Anal. Chim. Acta 853 (1) (2015) 1–18, https://doi.org/ 10.1016/J.ACA.2014.06.011.
- [73] Y. Shao, Y. Ying, J. Ping, Recent advances in solid-contact ion-selective electrodes: functional materials, transduction mechanisms, and development trends, Chem. Soc. Rev. 49 (13) (2020) 4405–4465, https://doi.org/10.1039/C9CS00587K.
- [74] K. Koirala, F.B. Sevilla, J.H. Santos, Biomimetic potentiometric sensor for chlorogenic acid based on electrosynthesized polypyrrole, Sensors Actuators B Chem. 222 (2016) 391–396, https://doi.org/10.1016/J.SNB.2015.08.084.
- [75] S.M. Oliveira, et al., High-performance electrochemical sensor based on molecularly imprinted polypyrrole-graphene modified glassy carbon electrode, Thin Solid Films 699 (2020), https://doi.org/10.1016/j.tsf.2020.137875.
- [76] V. Ratautaite, et al., Molecularly imprinted polypyrrole based sensor for the detection of SARS-CoV-2 spike glycoprotein, Electrochim. Acta 403 (2022), https://doi.org/10.1016/j.electacta.2021.139581.
- [77] C. Salvo-Comino, et al., Voltammetric sensor based on electrodeposited molecularly imprinted chitosan film on BDD electrodes for catechol detection in buffer and in wine samples, Mater. Sci. Eng. C 110 (2020), https://doi.org/ 10.1016/j.msec.2020.110667.
- [78] O. Gursoy, S. Sen Gursoy, S. Cogal, G. Celik Cogal, Development of a new two-enzyme biosensor based on poly(pyrrole-co-3,4-ethylenedioxythiophene) for lactose determination in milk, Polym. Eng. Sci. 58 (6) (2018) 839–848, https://doi.org/10.1002/pen.24632.
- [79] S. Aytac, F. Kuralay, I.H. Boyaci, C. Unaleroglu, A novel polypyrrole-phenylboronic acid based electrochemical saccharide sensor, Sensors Actuators B Chem. 160 (1) (2011) 405–411, https://doi.org/10.1016/j.snb.2011.07.069.
- [80] P. Bollella, et al., Green synthesis and characterization of gold and silver nanoparticles and their application for development of a third generation lactose biosensor, Electroanalysis 29 (1) (2017) 77–86, https://doi.org/10.1002/ ELAN.201600476:SUBPAGE:STRING:FULL.
- [81] O. Gürsoy, G. Çelik, S.Ş. Gürsoy, Electrochemical biosensor based on surfactant doped polypyrrole (PPy) matrix for lactose determination, J. Appl. Polym. Sci. 131 (9) (2014) 40200, https://doi.org/10.1002/APP.40200.
- [82] H. Wu, Electrochemical sensor based on ionic liquid for detection of lactose content in dairy products, J. Food Meas. Charact. 18 (1) (2024) 313–319, https://doi.org/ 10.1007/S11694-023-02181-3/TABLES/2.
- [83] J. Jin, Y. Ge, G. Zheng, Y. Cai, W. Liu, G. Hui, D-glucose, d-galactose, and d-lactose non-enzyme quantitative and qualitative analysis method based on cu foam electrode, Food Chem. 175 (2015) 485–493, https://doi.org/10.1016/J. FOODCHEM.2014.11.148.
- [84] J.J. Belbruno, Molecularly imprinted polymers, Chem. Rev. 119 (1) (2019) 94–119, https://doi.org/10.1021/ACS.CHEMREV.8B00171/ASSET/IMAGES/ LARGE/CR-2018-00171R 0010.JPEG.
- [85] R. Rajkumar, A. Warsinke, H. Möhwald, F.W. Scheller, M. Katterle, Analysis of recognition of fructose by imprinted polymers, Talanta 76 (5) (2008) 1119–1123, https://doi.org/10.1016/J.TALANTA.2008.05.022.



Cristina García Cabezón She is professor at the Engineers School of the University of Valladolid and is the co-head of the group UVASens dedicated to the development of electrochemical sensors for the analysis of foods. She obtained a Degree in Chemistry (U. Zaragoza, 1991) and obtained her PhD in Industrial Engineering from the U. of Valladolid (1998) where she is currently professor at the Department of Materials Science. For several years her research was dedicated to the study of the electrochemical behavior of metals and metal nanoparticles and she became an expert in electrochemistry. e main lines of research in the field of Materials Science and Engineering Scien

neering are: Corrosion, Porous Materials, Coatings. She has dedicated to the development of electrochemical sensors for the analysis of foods, where her skills in electrochemistry of metals and nanoparticles busted the research in the field of electronic tongues of the group. She has developed electrochemical sensors based on nanoparticles dedicated to the detection of antioxidants and the analysis in wines and milks. She is author or co-author of 65 indexed articles (H index 22). She serves a referee of several journals related to electrochemistry (electrochimica acta, corrosion science, sensors, etc.) she revers 5-10 papers per year. She regularly participates in contracts with industries.